Journal of Catalysis 263 (2009) 321–327

Contents lists available at ScienceDirect

Journal of Catalysis

www.elsevier.com/locate/jcat

Supported ionic liquid phase (SILP) catalyzed hydroformylation of 1-butene in a gradient-free loop reactor

Marco Haumann *, Michael Jakuttis, Sebastian Werner, Peter Wasserscheid

Lehrstuhl für Chemische Reaktionstechnik, Universität Erlangen-Nürnberg, Egerlandstr. 3, D-91058 Erlangen, Germany

ARTICLE INFO

Article history:
Received 21 November 2008
Revised 24 January 2009
Accepted 20 February 2009
Available online 19 March 2009

Keywords:
Hydroformylation
Ionic liquid
Immobilization
Support
Kinetics

ABSTRACT

The supported ionic liquid phase (SILP) catalysis technology was applied to gas-phase hydroformylation of 1-butene using sulfoxantphos **1** modified rhodium complexes. Kinetic experiments were performed in a fixed bed reactor and compared to a gradient-free gas-phase loop reactor (Berty type). The influence of substrate concentration, temperature and syngas pressure was determined. Data from fixed bed and Berty reactor were found to be in good agreement with respect to activation energy and reaction order. Ex-situ NMR studies of fresh and used SILP catalysts confirmed that the ligand remained intact after prolonged time on stream.

1. Introduction

The immobilization of precious homogeneous catalysts is a field of intense research and several concepts have been developed during the last two decades [1]. Basically two strategies can be found in literature; the immobilization of the homogeneous catalyst in a second phase (aqueous, fluorous, micellar, ionic liquid, supercritical CO_2) or the heterogenization of the homogeneous complex by means of attachment to a support [2]. The novel supported ionic liquid phase (SILP) technology makes use of both strategies by dissolving a homogeneous catalyst in an ionic liquid which itself is highly dispersed on the internal surface of a porous material as depicted in Fig. 1 [3]. The resulting ionic liquid catalyst film is only a few nanometers thick and allows complete utilization of ionic liquid and catalyst since the mass transport resistance from the gas into the liquid phase is minimized [4]. The very low volatility of the common ionic liquids allows these catalyst systems to be used in continuous gas phase processes and time on stream can exceed 700 h without deactivation of the catalyst [5].

However, from a reaction engineering perspective the kinetic data determined in a fixed bed reactor design at high conversions are falsified due to the concentration gradient of the substrate along the catalyst bed. In order to determine kinetic data from such an integral reactor either elaborate data analysis and parameter estimation or sampling along the reactor axis, normally accompanied by elaborate sampling procedures, are necessary. In contrast, in a gradient-free reactor the kinetic data can be determined directly from inflow and outflow values. For gas phase reactions, a reactor design can be applied as shown in Fig. 2 that has been introduced by Berty in 1974 [6].

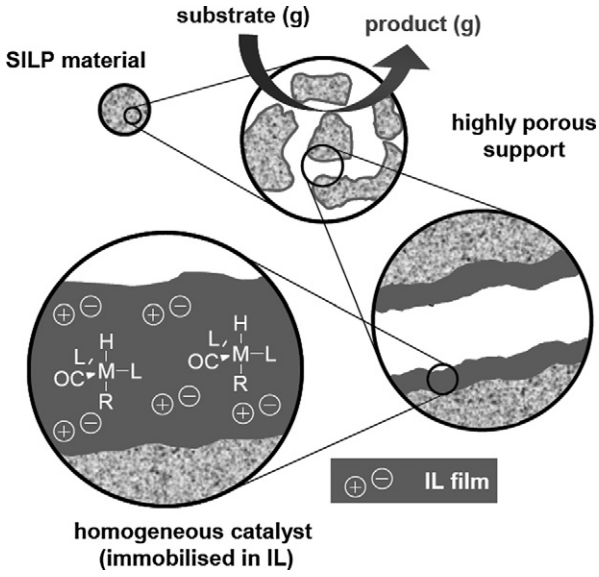

Fig. 1. Schematic representation of the heterogenization of a transition metal complex via supported ionic liquid phase (SILP) technology.

A turbine on top of the reactor vessel ensures circulation of the inlet flow through the catalyst bed, placed in a holder in the middle of the vessel. The circulating flow around the catalyst bed (loop flow) can be orders of magnitude higher than the flow through the

* Corresponding author. Fax: +49 9131 8527421.
E-mail address: marco.haumann@crt.cbi.uni-erlangen.de (M. Haumann).

0021-9517/$ – see front matter
doi:10.1016/j.jcat.2009.02.024

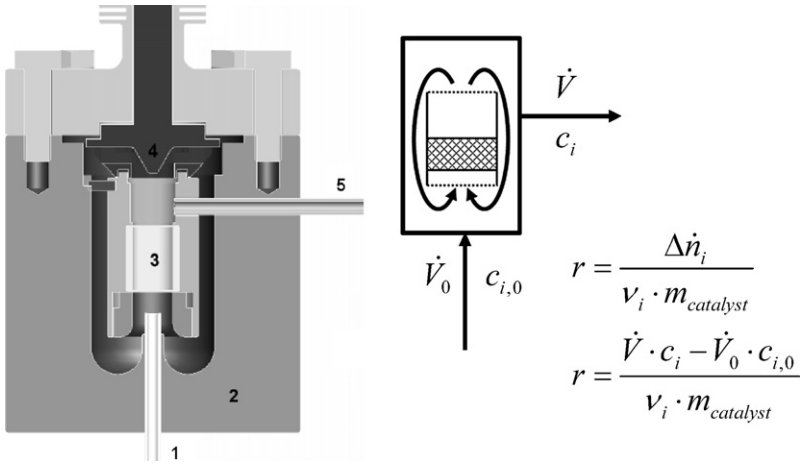

Fig. 2. Left: cross-section of a Berty reactor designed and manufactured in the workshop at CRT, Erlangen. 1: Reactor inlet; 2: reactor vessel; 3: catalyst basket; 4: turbine; 5: reactor outlet. Right: schematic representation of the flows inside the Berty reactor and resulting rate equation.

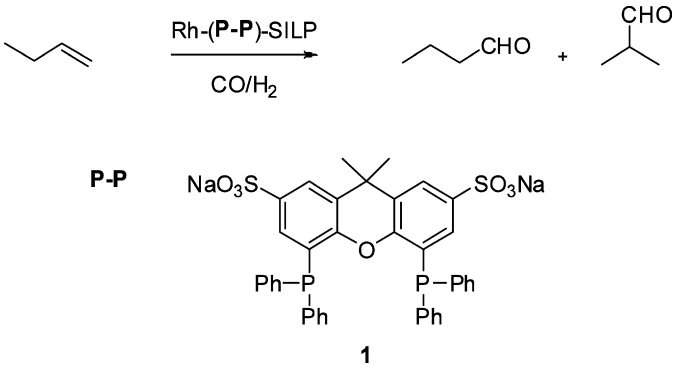

Scheme 1. Hydroformylation of 1-butene with sulfoxantphos **1** modified Rh-SILP catalysts.

catalyst bed, thus resulting in CSTR-like gradient-free concentration throughout the reactor. In such a system, the outlet concentration is representative for the concentration inside the catalyst bed and the kinetic data is not falsified by concentration gradients as given in Fig. 2.

We studied the hydroformylation of propene [3–5] and 1-butene [7] using rhodium based SILP catalysts in a fixed bed reactor. Interestingly, the catalyst activity with 1-butene as substrate was twice as high compared to propene under identical conditions [7]. This was attributed to the higher solubility of 1-butene, resulting in twice the substrate concentration in the ionic liquid film.

In order to investigate this higher activity in more detail, we studied the 1-butene hydroformylation with sulfoxantphos **1** modified rhodium complexes (Scheme 1) in a gradient-free loop reactor (Berty reactor) designed and manufactured in the Erlangen workshop.

2. Materials and methods

2.1. Chemicals

All syntheses were carried out using standard Schlenk techniques under argon (99.999%). $Rh(CO_2)(acac)$, xanthene and MeOH (HPLC grade) were purchased from Aldrich and used without further purification. The synthesis of sulfoxantphos ligand **1** was carried out according to literature procedures [8]. Silica gel 100 (63 to 200 µm) was purchased from Merck KGaA and was thermally pre-treated at 450 °C for 24 h. Carbon monoxide (99.97%), hydrogen (99.99%) and 1-butene (99.5%) were purchased from Linde AG. The ionic liquids were purchased from Solvent Innovation GmbH (now part of Merck KGaA). The water content was measured with Karl Fischer titration and the ionic liquids were dried under high vacuum at 50 °C overnight.

2.2. SILP catalyst preparation

0.0512 g (0.2 mmol) of $Rh(CO)_2(acac)$ was dissolved in 20 ml dried MeOH and stirred for 10 min. 1.57 g (2 mmol) of ligand sulfoxantphos was added and the orange solution was stirred for another 10 min. Afterward, 1 ml (1.06 g) of ionic liquid was added to the solution. After stirring for 30 min, 10 g calcined silica was added and the solution was stirred for 60 min. The MeOH was removed *in vacuo* and a pale red powder was obtained. The supported ionic liquid phase catalyst was stored under argon until further use.

2.3. Kinetic experiments

The continuous reactor setup (PFTR) for the SILP catalyzed hydroformylation has been described in detail previously [6]. The Berty reactor was in-house build and consisted of a 250 ml stainless steel vessel with a feed inlet at the bottom and an outlet at the side of the vessel. The catalyst basket is centered via three bolts into the middle of the reactor vessel. The turbine is fixed to the reactor lid and can thus be removed completely from the vessel for catalyst replacement. The supported ionic liquid phase (SILP) catalyst was filled into the reactor and the complete rig was evacuated at room temperature. The rig was pressurized with 50 bar helium and left under pressure for 30 min while monitoring the pressure. If no pressure drop was observed, the reactor was heated to reaction temperature under helium pressure. The complete setup was evacuated and flushed with helium three times before syngas and 1-butene were fed into the system. 1-butene was taken out of a reservoir in the liquid state and fed into a heated evaporator via a HPLC pump (Knauer WellChrom K-120, 10 ml min^{-1}) to control the molar flow of the substrate. Both carbon monoxide and hydrogen flows were adjusted by means of mass-flow controllers (MFC, 5850 S series, Brooks Instruments). The preheated gases were combined with the 1-butene in the mixing unit which was filled with glass beads in order to ensure proper mixing and isothermal conditions. The gas mixture could then either enter the reactor or exit the system via a bypass. A back pressure regulator valve (Samson Type 3277) was used to maintain the desired reaction pressure and outlet gas flow. After the regulator valve, the gas stream was split and a minor flow was passed through a 134 µl sampling loop mounted on a gas

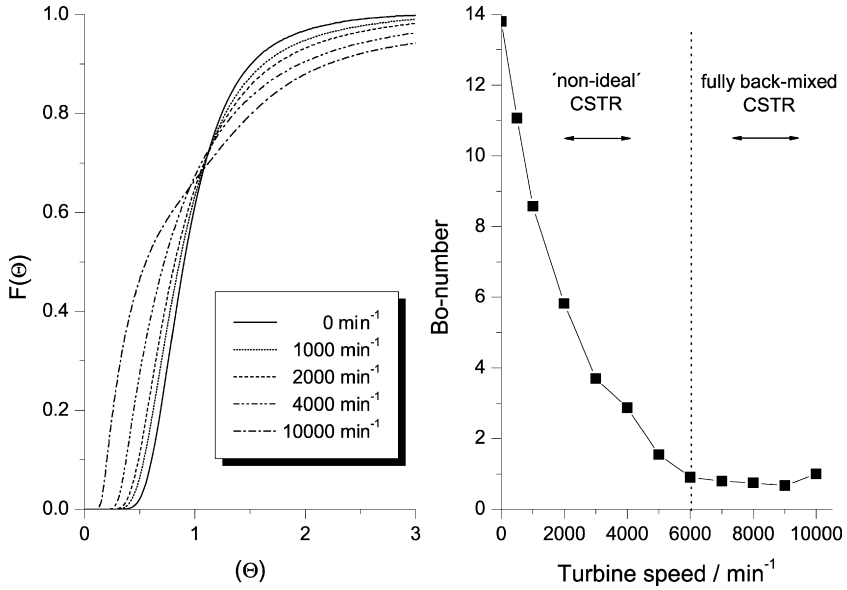

Fig. 3. Left: cumulative residence time function $F(\Theta)$ as a function of turbine speed. Right: dimensionless Bodenstein number as a function of turbine speed. 25 °C, atmospheric pressure, 175 ml min^{-1} helium flow, 250 µl pulse injection of propane.

chromatograph (HP 5890 II plus). Samples were taken at regular intervals by injecting the volume of the sampling loop via a 6-port valve (Vici AT60 series) into the GC.

2.4. Gas chromatography

The conversion of 1-butene as a function of process conditions was measured using on-line GC technique. A HP 5890 GC equipped with a Pona column (50 m, 0.2 mm diameter, 0.25 µm coating) and a flame ionization detector (FID) pre-calibrated for 1-butene, *n*-pentanal and iso-pentanal (allowing the peak areas to be transferred into 1-butene conversion) was applied: injector temperature 200 °C, split ratio 43:1, helium carrier gas flow 2.4 ml min^{-1}, detector temperature 250 °C. To detect possible high boiling by-products (heavies), the following temperature program was used: initial temperature 50 °C, initial time 5 min, heating ramp of 50 °C min^{-1}, final temperature 150 °C, final time 3 min, cooling ramp 50 °C min^{-1}, final temperature 50 °C.

2.5. NMR spectroscopy

The spectra of the fresh ligand solution and the solutions obtained by washing the SILP catalysts after reaction were analyzed in d_6-DMSO using a Jeol ECX 400 MHz spectrometer at room temperature. ^{31}P spectra were recorded at 161.8 MHz.

3. Results and discussion

3.1. Residence time distribution

In a first set of experiments, the Berty reactor was characterized with respect to the residence time distribution as a function of turbine speed and thus loop flow. The dimensionless residence time distribution function $E(\Theta)$ was calculated using a pulse function of propane at room temperature and under ambient pressure. The propane concentration in the exit flow was measured by IR (BINOS, Emerson Process Management GmbH). Transformation into the dimensionless cumulative RTD function $F(\Theta)$ was achieved by numerical integration. In Fig. 3 the results for turbine speeds between 0 and 10000 min^{-1} are shown.

Already at 0 min^{-1} the Berty reactor behaved significantly different from an ideal plug flow reactor (PFTR), probably due to some dead volume in the inlet and outlet tubing. With increasing turbine speed the behavior resembled an ideal back-mixed system of a CSTR. The dimensionless Bodenstein number was used as an indication of the degree of back-mixing in the reactor with $Bo = u_0 L/D_{ax}$ where u_0 is the flow velocity in the empty reactor, L is the reactor length and D_{ax} is the axial dispersion coefficient. According to literature procedure, the Bo-number was calculated from the slope of the graphs at the $\Theta = 1$ position [9]. Bodenstein numbers as a function of turbine speed are shown in the inlet of Fig. 3. Between 0 and 6000 min^{-1} a constant decrease of the Bodenstein number is observed, indicating a better degree of dispersion in the reactor. Between 6000 and 10000 min^{-1} a constant Bodenstein number of 1 was obtained. This low value is indicative of quasi-ideally back-mixed systems with no concentration gradient inside the reactor. All further experiments were conducted at 6000 min^{-1}. For an identical Berty setup the ideally back-mixed regime has been determined to start around 6000 min^{-1} in the hydrogenation of cyclohexene [10].

3.2. Residence time variation

Hydroformylation of 1-butene was studied at 100 °C and 10 bar total syngas pressure (CO/H_2 ratio 1:1). At 6000 min^{-1} the residence time inside the reactor was varied by changing the volume flow at the reactor inlet. For seven different values between 30 and 70 s the results are compiled in Fig. 4.

The conversion increased linear up to 20% with increasing residence time. At such low conversions this linear behavior can be expected. With higher conversion the selectivity decreased only slightly from 97.3% to 96.4% *n*-pentanal.

3.3. Temperature variation

For SILP catalysts the influence of reaction temperature was studied at 10 bar syngas pressure between 80 and 110 °C. The effective reaction rate r_{eff} increased with increasing temperature in an Arrhenius-type fashion. From a plot of $\ln r_{eff}$ versus T^{-1} the apparent activation energy was calculated to be 64.1 kJ mol^{-1} as shown in Fig. 5.

This value matches the activation energy of 63.8 kJ mol^{-1} for 1-butene hydroformylation determined in a PFTR setup under similar conditions [7]. This good agreement is not surprising, since the

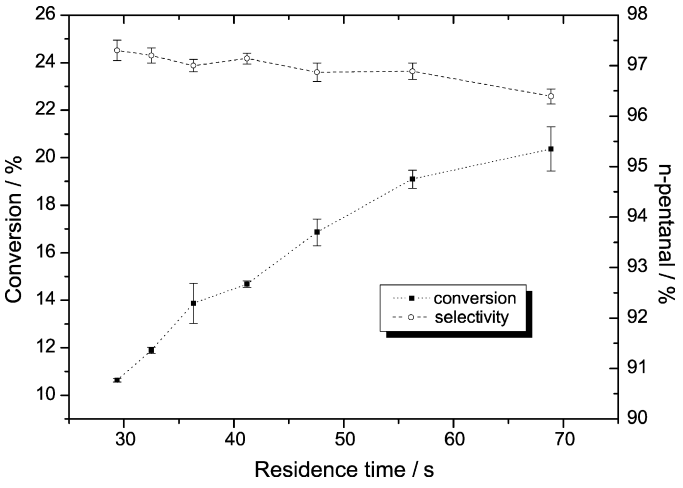

Fig. 4. Conversion and *n*-pentanal selectivity in SILP catalyzed hydroformylation of 1-butene as a function of residence time. 1.90 g SILP catalyst, $m_{Rh} = 0.2$ wt%, [BMIM][$C_8H_{17}OSO_3$], $\alpha = 0.1$, $p = 10$ bar, $T = 100\,^{\circ}C$, $\dot{V}_{CO} = 10.40$ N ml min^{-1}, $\dot{V}_{H_2} = 10.40$ N ml min^{-1}, $\dot{V}_{He} = 20$ N ml min^{-1}, $\dot{V}_{1\text{-butene,liq}} = 0.1$ ml min^{-1}. Error bars calculated from standard deviation of measured data points.

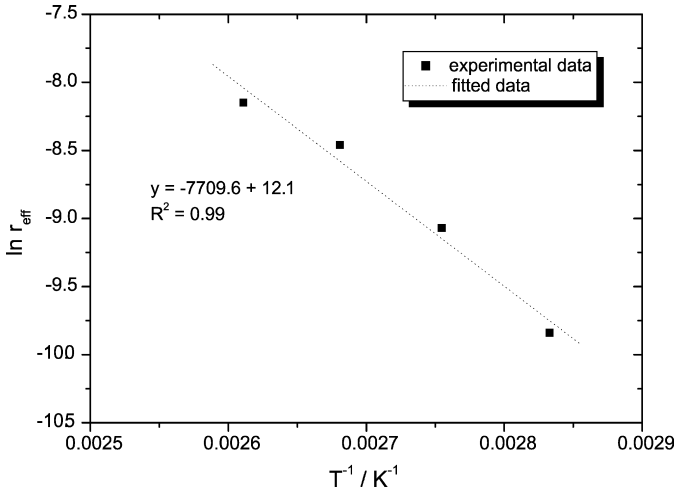

Fig. 5. Arrhenius plot of $\ln r_{eff}$ versus T^{-1} for the SILP catalyzed hydroformylation of 1-butene. 1.90 g SILP catalyst, $m_{Rh} = 0.2$ wt%, [BMIM][$C_8H_{17}OSO_3$], $\alpha = 0.1$, $p =$ 10 bar, $T = 80$ to $110\,^{\circ}C$, $\dot{V}_{CO} = 10.40$ N ml min^{-1}, $\dot{V}_{H_2} = 10.40$ N ml min^{-1}, $\dot{V}_{He} =$ 20 N ml min^{-1}, $\dot{V}_{1\text{-butene,liq}} = 0.1$ ml min^{-1}.

conversion was below 10% in the PFTR experiments, a prerequisite for the differential analysis of kinetic data.

3.4. Syngas composition variation

At 100 °C and 10 bar total pressure the syngas composition was varied. Fig. 6 shows the conversion and selectivity as a function of H_2:CO ratio.

The conversion increased from 11.6% at a 1:1 ratio to 13.3% at a 3:1 ratio. This behavior is well known from homogeneous catalysts and stems from the Wilkinson mechanism [11]. Formation of the active species $HRh(CO)(P_2)$ (P_2 = bisphosphine ligand) from $HRh(CO)_2(P_2)$ requires the loss of one CO, thus this step is hampered by high partial pressure of CO. On the other hand, reductive elimination of the aldehyde by H_2 from the 18e acyl species $H_2Rh(CO)(P_2)C(O)R$ is favored at high partial pressure of hydrogen. Upon further increase of the H_2:CO ratio the conversion decreased slightly to 12.5%. The selectivity was affected by the syngas composition and decreased linearly to a minor extend from 95.5% (1:1) to 94.4% (5:1). No hydrogenated by-products (pentanols) were detected under these conditions.

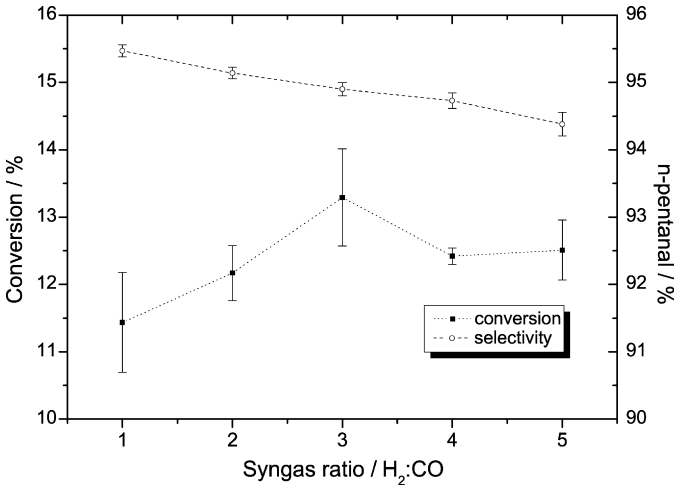

Fig. 6. Conversion and *n*-pentanal selectivity in SILP catalyzed hydroformylation of 1-butene as a function of syngas composition. 1.90 g SILP catalyst, $m_{Rh} = 0.2$ wt%, [BMIM][$C_8H_{17}OSO_3$], $\alpha = 0.1$, $p = 10$ bar, $T = 100\,^{\circ}C$, $\dot{V}_{1\text{-butene,liq}} = 0.1$ ml min^{-1}. Error bars calculated from standard deviation of measured data points.

3.5. Ex-situ NMR studies

The fate of the phosphine ligand immobilized on the SILP catalyst was investigated before and after the hydroformylation reaction by ex-situ NMR studies. Possible degradation can occur from oxidation according to Scheme 2. The intense signal for the fresh bisphosphine at −17.6 ppm (ca. 96%) indicated that the ligand was intact before any contact with the carrier. Only traces of mono oxidized ligand **2** were present, indicative by signals at −21.1 ppm and 25.7 ppm as shown in Fig. 7a.

The fresh ligand **1** was deliberately oxidized by treatment of a fresh solution of **1** with H_2O_2. This resulted in complete disappearance of the peak at −17.7 ppm while a strong signal at 30.7 ppm was obtained as shown in Fig. 7b. The intact ligand **1** was then used to prepare the SILP catalyst. After removal of the solvent, part of the prepared dry SILP material was washed with small amounts of ethanol in order to remove the ionic liquid film. Ethanol was removed from the solution *in vacuo* and the light red solution was analyzed in the NMR. The results for the ^{31}P NMR are shown in Fig. 7c.

The ^{31}P signal at −17.6 ppm was reduced in intensity to ca. 85% while the mono oxidized species **2** increased to more than 10%. A small doublet signal at 20.4 ppm with a coupling constant of $J_{Rh\text{-}P} = 99$ Hz was attributed to the dimeric rhodium species [Rh(μ-CO)(CO)(**1**)]$_2$ **4**, indicating that under these conditions enough ligand is left in the ionic liquid film to stabilize the rhodium precursor. Previous experiments have indicated that part of the ligand excess is irreversibly bound to the silica surface and that a ligand/rhodium ratio of 10 is required to compensate this loss [3d]. Beside the signals of free ligands **1** and **2** a small peak at 30.7 ppm was observed that indicated the double oxidized ligand **3**. This oxidation could either stem from oxygen impurity in the ethanol washing solution or from the SILP preparation itself. Since the same SILP catalyst batch showed excellent catalytic performance in the hydroformylation over 120 h time on stream, it is believed that the oxidation was rather due to the ethanol washing procedure. After 120 h time on stream the catalyst was removed from the Berty reactor and the ionic film was washed off with ethanol in a similar procedure as with the fresh catalyst but using more ethanol to allow all ionic liquid to be washed from the support. The same ^{31}P signals were obtained as shown in Fig. 7d except for the signal of the Rh-complex that are not visible any more due to the much higher dilution. Interestingly, in Fig. 7d the intensities has inversed compared to Fig. 7c with the mono

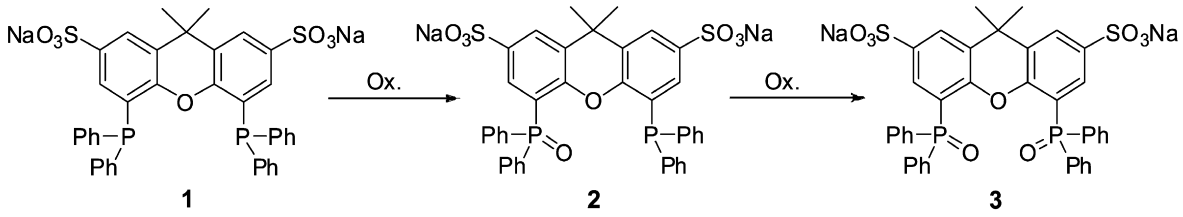

Scheme 2. Oxidation of the sulfoxantphos ligand 1 during the course of the SILP hydroformylation.

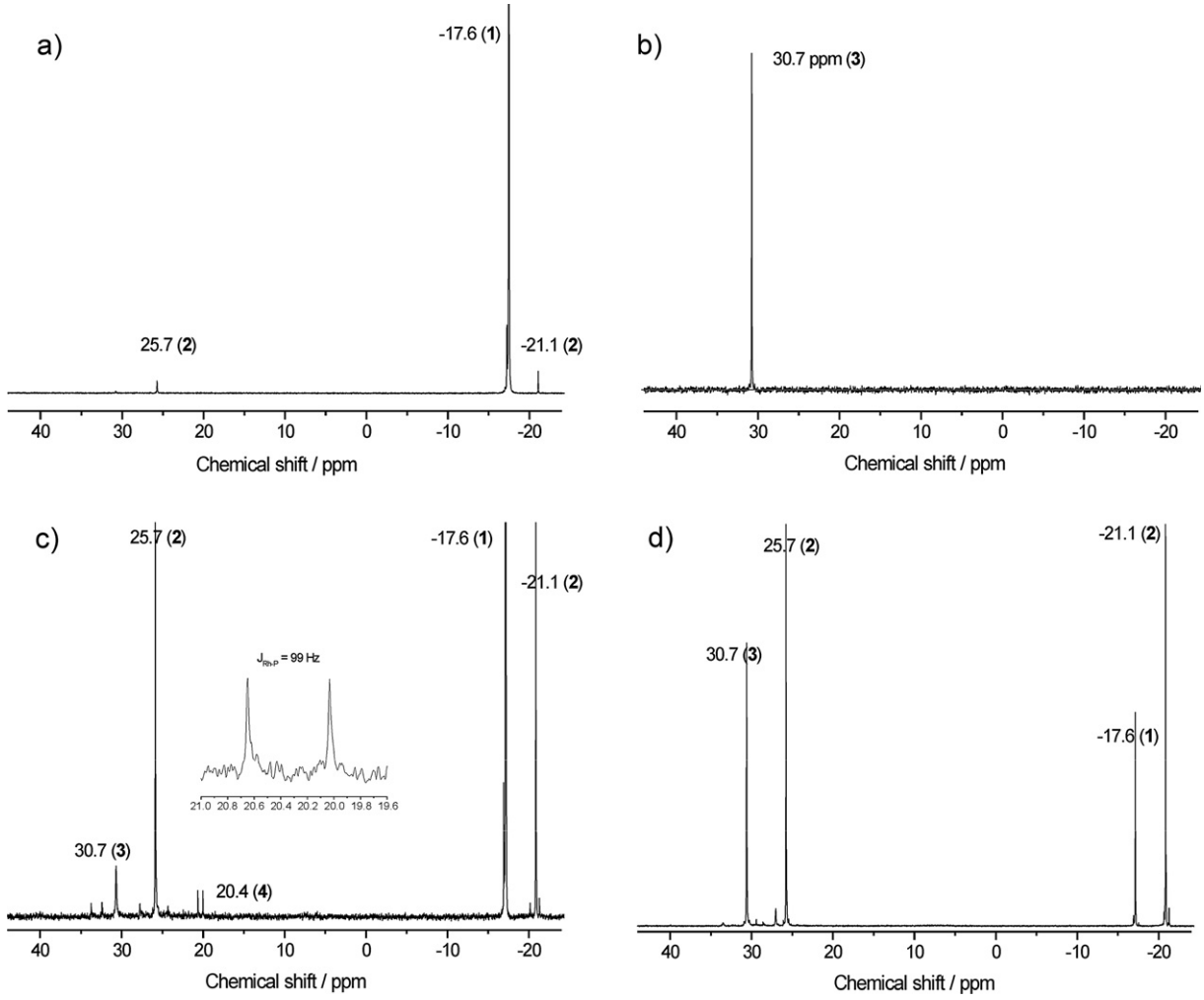

Fig. 7. ^{31}P NMR spectrum of fresh sulfoxantphos (a), fresh SILP catalyst after washing with EtOH (c) and used SILP catalyst after washing with a high amount of ethanol (d) in DMSO-d_6. Ionic liquid film and catalyst were washed from the SILP material with ethanol. Ethanol was removed *in vacuo* prior to NMR analysis. (b) shows a sample of the fresh ligand that was deliberately oxidized with H_2O_2 for a better comparison of the peak positions.

oxidized ligand **2** signal at −21.1 (42%) now being significantly larger than the one for the intact ligand at −17.6 ppm (18%). However, neither the partial oxidation of the sulfoxantphos ligand **1** nor the double oxidized ligand **3** at 30.4 ppm did influence the performance of the SILP catalyst, since the activity and selectivity remained high throughout the experiment. Experiments to verify the source of ligand oxidation are currently being conducted in our laboratory.

3.6. Influence of film or pore diffusion

Several criteria have been developed in order to estimate if the overall reaction is influenced by mass transport processes. By using the Mears criterion C_{Mears} one can account for film diffusion effects according to Eq. (1) [12].

$$C_{\text{Mears}} = \frac{r_{\text{eff}} \cdot \rho_{\text{cat}} \cdot \frac{d_p}{2} \cdot n}{c_{\text{bulk}} \cdot k_{\text{film}}} \leqslant 0.15. \quad (1)$$

The criterion includes the effective, mass related reaction rate r_{eff} [mol $\text{kg}_{\text{cat}}^{-1}$ s], the catalyst density ρ_{cat} [kg m^{-3}] and catalyst particle size d_p [m], the reaction order n, the bulk substrate concentration c_{bulk} [mol m^{-3}] and the diffusion rate constant k_{film} [m s^{-1}] through the film. At 130 °C and 10 bar the reaction rate r_{eff} was calculated from the molar substrate flow, the conversion and the catalyst mass according to Eq. (2).

$$r_{\text{eff}} = \frac{\dot{n} \cdot X}{m_{\text{cat}}} = 1.15 \times 10^{-3} \frac{\text{mol}}{\text{kg}_{\text{cat}}\,\text{s}}. \quad (2)$$

The Reynolds number *Re* was calculated to be 0.03 under the flow conditions applied (see Table 1).

Table 1
Parameters used for film and pore diffusion estimations.

Parameter	Symbol	Unit	Value
Temperature	T	°C	130
Pressure	p	bar	10
Particle diameter	d_p	m	1.32×10^{-5}
Viscosity of gas mixture[a]	$\bar{\nu}$	$m^2\,s^{-1}$	1.45×10^{-5}
Inner tube diameter	d_R	m	0.01
Gas velocity	u_0	$m\,s^{-1}$	3.28×10^{-3}
Reynolds number	Re		0.03
Molecular diffusion coefficient[b]	D_{12}	$m^2\,s^{-1}$	2.48×10^{-6}
Knudsen diffusion coefficient[c]	D_K	$m^2\,s^{-1}$	1.27×10^{-8}
Effective diffusion coefficient	D_{eff}	$m^2\,s^{-1}$	8.97×10^{-9}
Porosity	ε_P		0.9
Tortuosity[d]	τ		1.27
Film diffusion rate constant	k_{film}	$m\,s^{-1}$	1.20×10^{-4}
1-Butene molar flow	$\dot{n}$	$mol\,s^{-1}$	1.43×10^{-5}
1-Butene concentration	c_b	$mol\,m^{-3}$	55.64
1-Butene conversion	X		0.16
1-Butene molar mass	M_1	$kg\,kmol^{-1}$	56.11
Mass SILP catalyst	m_{cat}	kg	1.93×10^{-3}
Mass related effective reaction rate	r_{eff}	$mol\,kg_{cat}^{-1}\,s$	1.15×10^{-3}
Volume related effective reaction rate	r_{eff}	$mol\,m^{-3}\,s$	0.32
Density of catalyst bed	ρ_{cat}	$kg\,m^{-3}$	430
Mears criterion	C_M		4.75×10^{-3}
Weisz–Prater modulus	Φ_{WP}		1.11×10^{-2}
Thiele modulus	ϕ		0.11

[a] Average viscosity calculated from the viscosities of pure compounds (1-butene, H_2, CO, He) according to the gas composition.
[b] Calculated from a correlation by Hirschfelder et al. [15].
[c] Calculated from Eq. (7).
[d] Calculated according to a correlation by Dumanski [16].

The film diffusion rate constant k_{film} was calculated from the mass flow density J_{12} using correlations (3) and (4) [13,14].

$$J_{12} = 0.84 \cdot Re^{-0.51} = 5.04, \tag{3}$$

$$J_{12} = \frac{Sh}{Re \cdot Sc^{0.33}} = \frac{k_{film} \cdot \nu^{0.67}}{u_0 \cdot D_{12}^{0.67}}. \tag{4}$$

From the data given in Table 1 a film diffusion rate constant $k_{film} = 1.20 \times 10^{-4}\ m\,s^{-2}$ and a Mears criterion of $C_{Mears} = 0.0048$ were calculated. The C_{Mears}-value is more than 30 times smaller than the required Mears criterion limit. Under the conditions applied, film diffusion therefore has no influence on the SILP hydroformylation. The absence of film diffusion was further confirmed by the large value for the activation energy.

Pore diffusion influence was tested with the help of the Weisz–Prater criterion for spherical catalyst particles of diameter d_p, given by Eq. (5) for a first order reaction [17].

$$\Phi_{WP} = \frac{d_p^2}{4} \cdot \frac{r_{eff}}{D_{eff} \cdot c_b} \leqslant 1. \tag{5}$$

The effective diffusion coefficient for 1-butene was calculated from Eq. (6) assuming an interplay between molecular and Knudsen diffusion (Eq. (7)) inside the catalyst particle.

$$\frac{1}{D_{eff}} = \frac{\tau}{\varepsilon_P} \cdot \left(\frac{1}{D_{12}} + \frac{1}{D_K} \right), \tag{6}$$

$$D_K = 48.5 \cdot d_p \cdot \sqrt{\frac{T}{M_1}}. \tag{7}$$

From Eq. (5) a value for the Weisz–Prater modulus of $\Phi_{WP} = 0.0111$ was calculated. This extremely low value indicates the absence of pore diffusion limitation on the overall reaction rate. By rearranging Eq. (5) the maximum particle diameter was determined, when pore diffusion would begin to influence the overall reaction rate and thus the effectiveness factor of the SILP catalyst.

$$d_{p,max} \leqslant \sqrt{\frac{4 \cdot D_{eff} \cdot c_b}{r_{eff}}}. \tag{8}$$

Based on Eq. (8) a maximum particle diameter of 2.5 mm was calculated. This value is large enough for several forms of SILP catalysts to be applicable in a large scale hydroformylation process, e.g. as cylinders, pellets or extrudates.

Based on the small Weisz–Prater modulus, the effectiveness factor was assumed to be close to 1. The correlation between the Weisz–Prater modulus and the Thiele modulus for spherical particles is given in Eq. (9).

$$\phi^2 = \eta \cdot \Phi_{WP}. \tag{9}$$

Solving Eq. (8) for the Thiele modulus results in a value of $\phi = 0.11$.

4. Conclusion

In the present work we have applied a gradient-free gas phase reactor for the SILP catalyzed hydroformylation of 1-butene. The use of such a Berty type reactor allowed the determination of kinetic parameters without falsification from concentration or temperature gradients. At low conversions around 10% the activation energy has been determined between 80 and 110 °C to 64.1 $kJ\,mol^{-1}$, a value matching the result from fixed bed reactor studies under similar conditions. Furthermore, this value is large enough to account for absence of mass transport limitations from the gas into the ionic liquid phase. In order to test for limitation by film or pore diffusion, established criteria by Mears and Weisz–Prater have been applied. In both cases it was found that the SILP catalyst operates under no mass transport diffusion under the conditions applied. This is an important outcome of our studies with respect to possible application of the SILP technology for gas-phase hydroformylation reactions.

The stability of the SILP catalyst material was investigated by means of NMR in order to detect possible degradation products. No ligand degradation products could be found in the NMR spectra to a significant amount after 120 h time on stream. However, partial and complete oxidation of the ligand was observed in the NMR. Neither the partially nor the fully oxidized ligand seemed to lower the catalyst performance in terms of activity or selectivity significantly, thus it can be concluded that the oxidation occurred during NMR sample preparation.

We anticipate that the combination of SILP technology and Berty reactor design will provide fast and reliable insight into various homogeneously catalyzed reactions in the near future.

Acknowledgments

The authors would like to thank Michael Schmacks and Achim Mannke for help with the Berty setup. Dr. Peter Schulz is gratefully acknowledged for assistance with the NMR measurements. The authors would like to thank Dr. Robert Franke from Evonik Oxeno GmbH for fruitful discussions regarding the Mears and Weisz–Prater criteria.

References

[1] B. Cornils, W.A. Hermann, I.T. Horvath, W. Leitner, S. Mecking, H. Olivier-Bourbigou, D. Vogt (Eds.), Multiphase Homogeneous Catalysis, Wiley–VCH, Weinheim, 2005.
[2] D.J. Cole-Hamilton, Science 299 (2003) 1702.
[3] (a) C.P. Mehnert, R.A. Cook, N.C. Dispenziere, M. Afeworki, J. Am. Chem. Soc. 124 (2002) 12932;
(b) A. Riisager, K.M. Eriksen, P. Wasserscheid, R. Fehrmann, Catal. Lett. 90 (2003) 149;
(c) A. Riisager, P. Wasserscheid, R. van Hal, R. Fehrmann, J. Catal. 219 (2003) 252;

(d) A. Riisager, R. Fehrmann, S. Flicker, R. van Hal, M. Haumann, P. Wasserscheid, Angew. Chem. Int. Ed. 44 (2005) 185.
[4] A. Riisager, R. Fehrmann, M. Haumann, P. Wasserscheid, Eur. J. Inorg. Chem. (2006) 695.
[5] A. Riisager, R. Fehrmann, M. Haumann, B.S.K. Gorle, P. Wasserscheid, Ind. Eng. Chem. Res. 44 (2005) 9853.
[6] J. Berty, Chem. Eng. Prog. 70 (1974) 78.
[7] M. Haumann, K. Dentler, J. Joni, A. Riisager, P. Wasserscheid, Adv. Synth. Catal. 349 (2007) 425.
[8] M.S. Goedheijt, P.C.J. Kamer, P.W.N.M. van Leeuwen, J. Mol. Catal. A Chem. 134 (1998) 243.
[9] U. Pallaske, Chem. Ing. Tech. 56 (1984) 46.
[10] B. Etzold, A. Jess, University of Bayreuth, private communication.
[11] (a) J.F. Young, J.A. Osborn, F.A. Jardine, G. Wilkinson, J. Chem. Soc. Chem. Commun. (1965) 131;
(b) D. Evans, J.A. Osborn, G. Wilkinson, J. Chem. Soc. A (1968) 3133;
(c) D. Evans, G. Yagupsky, G. Wilkinson, J. Chem. Soc. A (1968) 2660.
[12] D.E. Mears, Ind. Eng. Chem. Process Des. Dev. 10 (1971) 541.
[13] O.A. Hougen, Ind. Eng. Chem. 53 (1961) 509.
[14] M. Baerns, H. Hofmann, in: M. Baerns, et al. (Eds.), Technische Chemie, Wiley–VCH, Weinheim, 2006.
[15] J.O. Hirschfelder, C.F. Curtiss, R.B. Bird, Molecular Theory of Gases, John Wiley & Sons, New York, 1967.
[16] A. von Dumanski, Kolloid Z. 3 (1908) 210.
[17] P.B. Weisz, Z. Phys. Chem. 11 (1957) 1.